



A Generalization for Model Reference Adaptive Control and Robust Model Reference Adaptive Control Adaptive Laws for a Class of Nonlinear Uncertain Systems with Application to Control of Wing Rock Phenomenon

J. Roshanian, E. Rahimzadeh*

Department of Aerospace Engineering, K.N. Toosi University of Technology, Tehran, Iran

PAPER INFO

Paper history:

Received 16 June 2020

Received in revised form 30 June 2020

Accepted 03 August 2020

Keywords:

Lyapunov's Direct Method

Model Reference Adaptive Control

Robust Model Reference Adaptive Control

General Adaptive Laws

Strictly Increasing Function

Wing Rock

ABSTRACT

Lyapunov's direct method is a primary tool for designing Model Reference Adaptive Control (MRAC) and robust MRAC schemes. In general, Lyapunov function candidates contain two categories of quadratic terms. The first category includes the system tracking error quadratic terms or, in some cases, consist of the system state quadratic terms. The second consists of the parameter estimation error quadratic terms. To design MRAC and Robust MRAC systems, researchers have used a limited variety for choosing quadratic terms. In this study, we consider a general form for the tracking error quadratic terms. We consider a strictly increasing function that belongs to the class of c^1 , which is a function of state tracking error quadratic terms. It yields a general structure for stable adaptive laws for updating controller parameters. For the MRAC scheme, the global asymptotic stability of the closed-loop system and stability and uniform bounded tracking of robust MRAC schemes are guaranteed. To evaluate the performance of the designed controllers, we consider the single DOF wing rock dynamics.

doi: 10.5829/ije.2020.33.11b.28

1. INTRODUCTION

Many combat aircraft may have to fly at a high angle of attack to obtain air superiority. In this situation, the flight occurs outside of the flight envelope in the nonlinear regime. In this situation, airflow separation may occur. In this situation, the boundary layer's speed relative to the wing is reduced to zero because the boundary layer moves against an adverse pressure gradient. When the aircraft moves through the air, cause the fluid flow to separate from the wing, and vortices are produced. The Wing Rock phenomenon is one of the undesirable motions which appears as limit cycle oscillations in the aircraft roll angle, leading to lateral directional instability and putting the flight in danger. Several experiments and investigations performed on a highly slender forebody and a highly swept delta wing. These studies confirmed that the interaction between the forebody and the wing vortices are the main cause of the wing rock motion [1-

10]. The exact analytical expression of the rolling moment coefficient is difficult to derive. Therefore, some researchers proposed several approximate models. A nonlinear aerodynamic model is proposed by Hsu and Lan [11] to drive the limit cycle amplitude and frequency of wing rock motion. based on the numerical simulation of the wing rock motion, an analytic expression for the roll moment coefficient is proposed by Nayfeh et al. [12]. The result was used to describe the phase plane analysis of the nonlinear motion, includes determining the type of equilibrium points and calculating domains of initial conditions that lead to oscillatory motion or divergence. A modified version of the wing rock model proposed by Hsu and Lan [11] is developed by Elzebdia et al. [13]. The numerical values of the coefficients, in the roll moment coefficient, are obtained by the curve fitting method. Data are collected from simulation results. The dynamical equations of motion of wing rock for aircraft,

*Corresponding Author Institutional Email: e.rahimzadeh@kntu.ac.ir
(E. Rahimzadeh)

which have single, two, and three rotational degrees of freedom, are proposed by Go [14].

The control of the wing rock is a significant research area and a series of studies based on the control methods presented in what follows. A neural-network identification based control (NNIAC) scheme using the L2 tracking technique is developed to reduce the effect of the approximation error on the tracking performance [15]. The proposed controller is applied to control a wing rock limit cycle to show its effectiveness. It has been reported in literature [16], a new reinforcement adaptive fuzzy control system for tracking control a wing rock motion in the presence of the uncertainty and unknown Elzebda is proposed. A fuzzy approximator is applied to identify the unknown nonlinear function. The reinforcement adaptive law derived from the Lyapunov stability theory. The proposed algorithm showed high tracking performance and robustness in the presence of uncertainty [17]. A simplified interval fuzzy sliding control scheme is proposed for suppressing and tracking the desired trajectories. The simulation results showed that the proposed algorithm could make the wing rock system reach the desired state without overshoots. A supervisory recurrent fuzzy neural network control (SRFNCC) system is proposed for the wing rock control system [18]. An adaptive feedback linearizing controller with the backstepping approach for the wing rock control is proposed in literature [19]. A new control law based on the variable structure model reference adaptive control is presented [20]. The wing rock problem with unstructured nonlinearity and disturbance input is considered. Simulation results showed good transient performance and disturbance rejection capability of the proposed controller.

The Lyapunov stability method, also known as the Lyapunov's direct method, is widely used in the design of adaptive algorithms for updating controller parameters or designing adaptive observers. An SM rotor flux observer has been developed to estimate rotor speed [21]. The stability of this observer is guaranteed by the Lyapunov's stability method. A new method for designing adaptive fuzzy dynamic sliding mode control for the nonlinear system is applied [22]. The process of deriving adaptive switching gain is performed by Lyapunov's direct method. A new adaptive control for direct-drive robot manipulators driven by PMSM in tracking application has been developed [23]. The control method has verified by the Lyapunov stability method. A robust adaptive controller is implemented to control a spacecraft simulator [24]. The proposed controller is designed based on nonlinear dynamics to overcome of model uncertainty. The stability of the robust adaptive controller is verified through Lyapunov's theorem. An observer-based robust controller with an adaptive mechanism designed by Lyapunov's method is proposed to control a robotic system [25]. A fuzzy adaptive sliding mode

controller was derived for a class of multi-agent systems [26]. The stability of the closed-loop system is verified by Lyapunov's method. Quadratic Lyapunov functions are widely applied in the analysis of linear and nonlinear systems and the design of adaptive systems. One of the methods of designing adaptive systems is based on Lyapunov's stability method, which is widely used in designing stable MRAC systems. By using a new non-quadratic Lyapunov function (NQLF), new adaptive Laws for the MRAC scheme presented in literature [27]. The author used e^4 instead of e^2 signal for the tracking error, in the Lyapunov function and the new stable adaptive laws which contain e^3 signal derived. By using the same Lyapunov function, new adaptive law which uses the cube of the same error signal for robust adaptive scheme, dead zone modification, is presented [28]. A control scheme for the robust adaptive tracking based on MRAC via a switching non-quadratic Lyapunov function is proposed [29]. In this study, we intend to design the MRAC and Robust MRAC controller by considering a general form for the Lyapunov function candidate. In section (2), we introduce the mathematical model of the wing rock proposed in literature [13]. In the section (3) we design MRAC with Matched parameter uncertainty with a general Lyapunov function candidate, In the section (4) we design MRAC modifications known as sigma modification and e-modification with the Lyapunov function introduced in section (3) and in the section (5) some simulations have done to evaluate the performance of the MRAC and Robust MRAC designed in the previous sections.

2. WING ROCK DYNAMICS AND PHASE PLANE ANALYSIS

The wing rock phenomenon happens in the six DOF space, but the dominant feature of this motion can be demonstrated by a one DOF oscillation along the longitudinal axis of aircraft. The mathematical models of the wing rock presented in the literature were obtained by the least-square fitting method in the data of the wind tunnel test. In this section, we introduce the one DOF roll moment coefficient, the modified Hsu and Lan model, studied by Elzebda et al. [13]:

$$C_L(\phi(t), \dot{\phi}(t)) = a_1\phi(t) + a_2\dot{\phi}(t) + a_3|\phi(t)|\dot{\phi}(t) + a_4|\dot{\phi}(t)|\dot{\phi}(t) + a_5\phi^3(t) \quad (1)$$

In Equation (1), $\phi(t)$ is the roll angle, $\dot{\phi}(t)$ is the roll rate, and a_i are the roll moment coefficients obtained by fitting this expression to the numerical simulation gathered from wind tunnel test using the least square criteria. The following equation of motion is considered in literature [12-13]:

$$\ddot{\phi}(t) = \frac{\rho U_{\infty}^2 S b}{2I_{xx}} C_L(\phi(t), \dot{\phi}(t)) + D\dot{\phi}(t) \quad (2)$$

In Equation (2), ρ is the air density, S is the plan form area, U_∞ is the freestream speed, b is the chord, and I_{xx} is the wing mass moment of inertia around the midspan axis. The effect of bearing viscous damping presented by the last term. Let:

$$E = \frac{\rho U_\infty^2 S b}{2 I_{xx}} \tag{3}$$

Substituting Equation (2) into Equation (1) yields:

$$\ddot{\phi}(t) = E a_1 \phi(t) + (E a_2 + D) \dot{\phi}(t) + E a_3 |\phi(t)| \dot{\phi}(t) + E a_4 |\dot{\phi}(t)| \phi(t) + E a_5 \phi^3(t) \tag{4}$$

The values of E and the viscous damping coefficient, D is considered as [13]:

$$E = 0.354 \tag{5}$$

$$D = 0.001 \tag{6}$$

The values of the roll moment coefficients a_i , in the Equation (1) for different angles of attack are presented in Table 1.

Considering the initial condition $\phi(0) = 1$ (deg), $\dot{\phi}(0) = 0$ ($\frac{\text{deg}}{\text{sec}}$), and Angle of attack $\alpha = 22.5$ deg the uncontrolled motion of the wing rock phenomenon is presented in the Figures 1 to 4.

According to Figures 1 to 4, it is clear that although the initial condition is small, the roll angle develops into the limit cycle, which means that a small disturbance is sufficient to cause the wing rock oscillation. The mathematical control model for a single DOF wing rock phenomenon is considered as follows:

TABLE 1. Coefficients of Equation (1) [13]

$\alpha(\text{deg})$	a_1	a_2	a_3	a_4	a_5
15	-0.010259	-0.02143	0.05711	-0.0619	-0.146
21.5	-0.04177	0.01461	-0.06732	0.0841	0.046
22.5	-0.04569	0.02351	-0.09944	0.0689	0.0531
25	-0.05256	0.04568	-0.1765	0.0269	0.0606

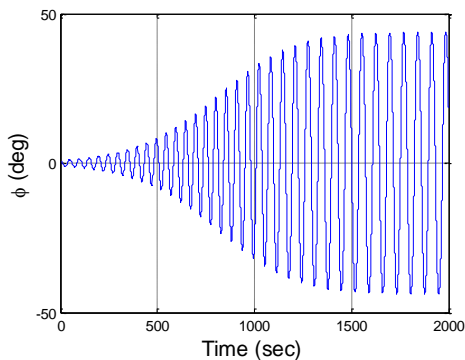


Figure 1. Roll Angle Limit Cycle build up $\alpha = 22.5$ deg

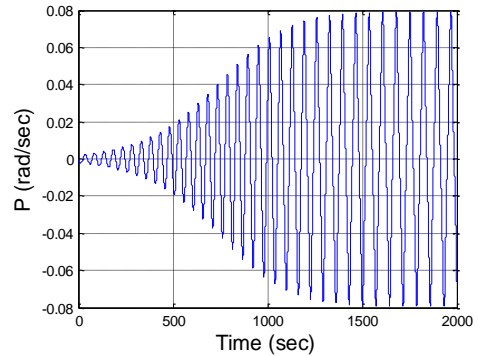


Figure 2. Roll Rate Limit Cycle build up $\alpha = 22.5$ deg

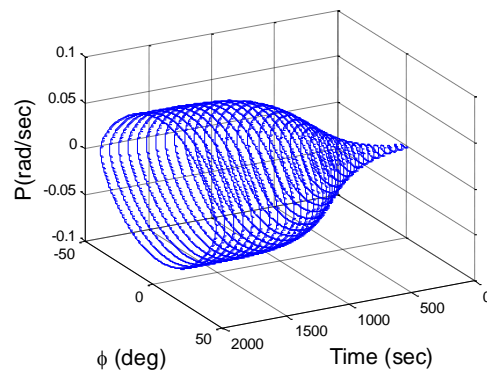


Figure 3. Wing Rock Limit Cycle $\alpha = 22.5$ deg

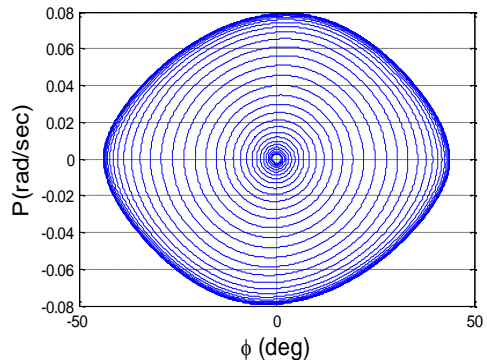


Figure 4. Wing Rock Phase Plane $\alpha = 22.5$ deg

$$\ddot{\phi} = E C_1 + D \dot{\phi} + d_0 u \tag{7}$$

In Equation (7), d_0 is the control effectiveness, and u is the control signal. Let $x_1 = \phi$, $x_2 = \dot{\phi}$. The state-space representation of Equation (2) becomes:

$$\begin{aligned} \dot{x}_1 &= x_2 \\ \dot{x}_2 &= E a_1 x_1 + (E a_2 + D) x_2 + E a_3 |x_1| x_2 + E a_4 |x_2| x_2 + E a_5 x_1^3 + d_0 u \end{aligned} \tag{8}$$

Equation (8) can be written in the matrix form as follows:

$$\begin{bmatrix} \dot{x}_1(t) \\ \dot{x}_2(t) \end{bmatrix} = \begin{bmatrix} 0 & 1 \\ E a_1 & E a_2 + D \end{bmatrix} \begin{bmatrix} x_1(t) \\ x_2(t) \end{bmatrix} + \begin{bmatrix} 0 \\ 1 \end{bmatrix} d_0(u + \frac{E a_3}{d_0} |x_1| x_2 + \frac{E a_4}{d_0} |x_2| x_2 + \frac{E a_5}{d_0} x_1^3(t)) \quad (9)$$

3. MRAC DESIGN FOR MIMO SYSTEMS WITH MATCHED UNCERTAINTY

In this section, we design an MRAC controller with general stable adaptive laws for a class of nonlinear systems with parametric uncertainty. We consider a MIMO system in the form of Equation (10):

$$\dot{x}(t) = Ax(t) + B\Lambda(u(t) + M(x(t))) \quad (10)$$

where in Equation (10), $x(t) \in \mathbb{R}^n$ is the system state vector, $A \in \mathbb{R}^{n \times n}$ is supposed to be constant and unknown, $B \in \mathbb{R}^{n \times m}$ is constant and known, $\Lambda \in \mathbb{R}^{m \times m}$ is an unknown constant matrix, and it is supposed to be diagonal with strictly positive elements, $u(t) \in \mathbb{R}^m$ is the control input, we assume that the pair $(A, B\Lambda)$ is controllable. In general, $M(x(t)): \mathbb{R}^n \rightarrow \mathbb{R}^m$ is an unknown vector function which its components are functions of $x(t)$, it is supposed that $M(x(t))$ could be written in the form of Equation (11):

$$M(x(t)) = \theta^T(t)\mu(x(t)) \quad (11)$$

In Equation (11), $\theta(t) \in \mathbb{R}^{N \times m}$ is an unknown matrix with constant coefficients, and $\mu(x(t)) \in \mathbb{R}^N$ is an N-dimensional regressor vector:

$$\mu(x(t)) = (\mu_1(x(t)), \mu_2(x(t)), \mu_3(x(t)), \dots, \mu_N(x(t)))^T \quad (12)$$

Equation (11) represents the matched parametric uncertainty of the system. We consider the following reference model:

$$\dot{x}_m(t) = A_m x_m(t) + B_m r(t) \quad (13)$$

In Equation (13), A_m is a model reference Hurwitz matrix, and $r(t)$ is a bounded reference command. We consider the following definition:

$$\tilde{x}(t) = x(t) - x_m(t) \quad (14)$$

Without having parametric uncertainty which means that A and Λ are known, we use the following ideal fixed gain control law:

$$u(t) = K_x^T x(t) + K_r^T r(t) - \theta^T \mu(x(t)) \quad (15)$$

Using Equations (15) and (10), yields:

$$\dot{x}(t) = Ax(t) + B\Lambda[K_x^T x(t) + K_r^T r(t)] = (A + B\Lambda K_x^T)x(t) + B\Lambda K_r^T r(t) \quad (16)$$

Assumption: Given matrices A and B and an unknown matrix Λ , there must exist unknown matrices K_x and K_r must satisfy Equation (17):

$$A_m = A + B\Lambda K_x^T, \quad B_m = B\Lambda K_r^T \quad (17)$$

Now control input is chosen as follows:

$$u(t) = \hat{K}_x^T(t)x(t) + \hat{K}_r^T(t)r(t) - \hat{\theta}^T(t)\mu(x(t)) \quad (18)$$

Using Equations (18), (10), and (11) yields:

$$\dot{x}(t) = (A + B\Lambda \hat{K}_x^T(t))x(t) + B\Lambda(\hat{K}_r^T(t)r(t) - (\hat{\theta}(t) - \theta)^T \mu(x(t))) \quad (19)$$

Subtracting Equation (13) from Equation (19), yields:

$$\dot{\tilde{x}} = (A + B\Lambda \hat{K}_x^T(t))\tilde{x}(t) + B\Lambda(\hat{K}_r^T(t)r(t) - (\hat{\theta}(t) - \theta)^T \mu(x(t)) - A_m x_m(t) - B_m r(t)) \quad (20)$$

Using Equation (17), Equation (20) becomes:

$$\dot{\tilde{x}}(t) = A_m \tilde{x}(t) + B\Lambda[(\hat{K}_x(t) - K_x)^T \tilde{x}(t) + (\hat{K}_r(t) - K_r)^T r(t) - (\hat{\theta}(t) - \theta)^T \mu(x(t))] \quad (21)$$

The parameter estimation errors are defined as follows:

$$\begin{cases} \tilde{\theta}(t) = \hat{\theta}(t) - \theta \\ \tilde{K}_x(t) = \hat{K}_x(t) - K_x \\ \tilde{K}_r(t) = \hat{K}_r(t) - K_r \end{cases} \quad (22)$$

Substituting Equation (22) into Equation (21) yields the tracking error dynamics:

$$\dot{\tilde{x}}(t) = A_m \tilde{x}(t) + B\Lambda[\tilde{K}_x^T(t)\tilde{x}(t) + \tilde{K}_r^T(t)r(t) - \tilde{\theta}^T(t)\mu(x(t))] \quad (23)$$

We consider a general quadratic Lyapunov function candidate in the form of Equation (24):

$$V = f(\tilde{x}^T(t)P\tilde{x}(t)) + \text{tr}([\tilde{K}_x^T(t)\Gamma_x^{-1}\tilde{K}_x(t) + \tilde{K}_r^T(t)\Gamma_r^{-1}\tilde{K}_r(t) + \tilde{\theta}^T(t)\Gamma_\theta^{-1}\tilde{\theta}(t)]\Lambda) \quad (24)$$

In Equation (24), f is a scalar function, which is strictly increasing $f' > 0$ with $f(0)=0$, and it is supposed to be continuously differentiable ($f \in C^1$). Γ_x , Γ_r , and Γ_θ are symmetric positive definite matrices denote the rates of adaptation. P is the symmetric positive definite matrix which is the unique solution of the algebraic Lyapunov equation with symmetric positive definite matrix Q :

$$A_m^T P + P A_m = -Q \quad (25)$$

The first time derivative of the Lyapunov function becomes:

$$\dot{V} = \frac{df(\tilde{x}^T(t)P\tilde{x}(t))}{dt} + 2\text{tr}([\tilde{K}_x^T(t)\Gamma_x^{-1}\dot{\tilde{K}}_x(t) + \tilde{K}_r^T(t)\Gamma_r^{-1}\dot{\tilde{K}}_r(t) + \tilde{\theta}^T(t)\Gamma_\theta^{-1}\dot{\tilde{\theta}}(t)]\Lambda) \quad (26)$$

Using the chain rule for simplifying the time derivative yields:

$$\dot{V} = \frac{df(\tilde{x}^T(t)P\tilde{x}(t))}{d(\tilde{x}^T(t)P\tilde{x}(t))} \frac{d(\tilde{x}^T(t)P\tilde{x}(t))}{dt} + 2\text{tr}([\tilde{K}_x^T(t)\Gamma_x^{-1}\dot{\tilde{K}}_x(t) + \tilde{K}_r^T(t)\Gamma_r^{-1}\dot{\tilde{K}}_r(t) + \tilde{\theta}^T(t)\Gamma_\theta^{-1}\dot{\tilde{\theta}}(t)]\Lambda) \quad (27)$$

The first term of Equation (27) can be written as follows:

$$\begin{aligned} \dot{V} = & (\dot{\tilde{\mathbf{x}}}(t)\mathbf{P}\tilde{\mathbf{x}}(t) + \tilde{\mathbf{x}}^T(t)\mathbf{P}\dot{\tilde{\mathbf{x}}}(t)) \frac{d(\tilde{\mathbf{x}}^T(t)\mathbf{P}\tilde{\mathbf{x}}(t))}{d(\tilde{\mathbf{x}}^T(t)\mathbf{P}\tilde{\mathbf{x}}(t))} + \\ & 2\text{tr}\left[\tilde{\mathbf{K}}_x^T(t)\Gamma_x^{-1}\dot{\tilde{\mathbf{K}}}_x(t) + \tilde{\mathbf{K}}_r^T(t)\Gamma_r^{-1}\dot{\tilde{\mathbf{K}}}_r(t) + \right. \\ & \left. \tilde{\boldsymbol{\theta}}^T(t)\Gamma_\theta^{-1}\dot{\tilde{\boldsymbol{\theta}}}(t)\right]\boldsymbol{\Lambda} \end{aligned} \quad (28)$$

Evaluating Equation (28) along the trajectory of the error dynamics Equation (23) yields:

$$\begin{aligned} \dot{V} = & -(\tilde{\mathbf{x}}^T(t)\mathbf{Q}\tilde{\mathbf{x}}(t)) \frac{d(\tilde{\mathbf{x}}^T(t)\mathbf{P}\tilde{\mathbf{x}}(t))}{d(\tilde{\mathbf{x}}^T(t)\mathbf{P}\tilde{\mathbf{x}}(t))} + \\ & 2\tilde{\mathbf{x}}^T(t)\mathbf{PBA}\tilde{\mathbf{K}}_x^T(t)\mathbf{x}(t) \frac{d(\tilde{\mathbf{x}}^T(t)\mathbf{P}\tilde{\mathbf{x}}(t))}{d(\tilde{\mathbf{x}}^T(t)\mathbf{P}\tilde{\mathbf{x}}(t))} + \\ & 2\tilde{\mathbf{x}}^T(t)\mathbf{PBA}\tilde{\mathbf{K}}_r^T(t)\mathbf{r}(t) \frac{d(\tilde{\mathbf{x}}^T(t)\mathbf{P}\tilde{\mathbf{x}}(t))}{d(\tilde{\mathbf{x}}^T(t)\mathbf{P}\tilde{\mathbf{x}}(t))} - \\ & 2\tilde{\mathbf{x}}^T(t)\mathbf{PBA}\tilde{\boldsymbol{\theta}}^T(t)\boldsymbol{\mu}(\mathbf{x}(t)) \frac{d(\tilde{\mathbf{x}}^T(t)\mathbf{P}\tilde{\mathbf{x}}(t))}{d(\tilde{\mathbf{x}}^T(t)\mathbf{P}\tilde{\mathbf{x}}(t))} + \\ & 2\text{tr}\left[\left[\tilde{\mathbf{K}}_x^T(t)\Gamma_x^{-1}\dot{\tilde{\mathbf{K}}}_x(t) + \tilde{\mathbf{K}}_r^T(t)\Gamma_r^{-1}\dot{\tilde{\mathbf{K}}}_r(t) + \right. \right. \\ & \left. \left. \tilde{\boldsymbol{\theta}}^T(t)\Gamma_\theta^{-1}\dot{\tilde{\boldsymbol{\theta}}}(t)\right]\boldsymbol{\Lambda} \right) \end{aligned} \quad (29)$$

Applying the vector-trace identity:

$$\mathbf{w}^T\mathbf{z} = \text{tr}(\mathbf{z}\mathbf{w}^T) \quad (30)$$

Yields:

$$\begin{aligned} \tilde{\mathbf{x}}^T(t)\mathbf{PBA}\tilde{\mathbf{K}}_x^T(t)\mathbf{x}(t) \frac{d(\tilde{\mathbf{x}}^T(t)\mathbf{P}\tilde{\mathbf{x}}(t))}{d(\tilde{\mathbf{x}}^T(t)\mathbf{P}\tilde{\mathbf{x}}(t))} = \\ \text{tr}\left(\tilde{\mathbf{K}}_x^T(t)\mathbf{x}(t)\tilde{\mathbf{x}}^T(t)\mathbf{PBA} \frac{d(\tilde{\mathbf{x}}^T(t)\mathbf{P}\tilde{\mathbf{x}}(t))}{d(\tilde{\mathbf{x}}^T(t)\mathbf{P}\tilde{\mathbf{x}}(t))}\right) \\ \tilde{\mathbf{x}}^T(t)\mathbf{PBA}\tilde{\mathbf{K}}_r^T(t)\mathbf{r}(t) \frac{d(\tilde{\mathbf{x}}^T(t)\mathbf{P}\tilde{\mathbf{x}}(t))}{d(\tilde{\mathbf{x}}^T(t)\mathbf{P}\tilde{\mathbf{x}}(t))} = \\ \text{tr}\left(\tilde{\mathbf{K}}_r^T(t)\mathbf{r}(t)\tilde{\mathbf{x}}^T(t)\mathbf{PBA} \frac{d(\tilde{\mathbf{x}}^T(t)\mathbf{P}\tilde{\mathbf{x}}(t))}{d(\tilde{\mathbf{x}}^T(t)\mathbf{P}\tilde{\mathbf{x}}(t))}\right) \\ \tilde{\mathbf{x}}^T(t)\mathbf{PBA}\tilde{\boldsymbol{\theta}}^T(t)\boldsymbol{\mu}(\mathbf{x}(t)) \frac{d(\tilde{\mathbf{x}}^T(t)\mathbf{P}\tilde{\mathbf{x}}(t))}{d(\tilde{\mathbf{x}}^T(t)\mathbf{P}\tilde{\mathbf{x}}(t))} = \\ \text{tr}\left(\tilde{\boldsymbol{\theta}}^T(t)\boldsymbol{\mu}(\mathbf{x}(t))\tilde{\mathbf{x}}^T(t)\mathbf{PBA} \frac{d(\tilde{\mathbf{x}}^T(t)\mathbf{P}\tilde{\mathbf{x}}(t))}{d(\tilde{\mathbf{x}}^T(t)\mathbf{P}\tilde{\mathbf{x}}(t))}\right) \end{aligned} \quad (31)$$

Using Equations (29) and (31) and Collecting similar terms gives:

$$\begin{aligned} \dot{V} = & -\tilde{\mathbf{x}}^T(t)\mathbf{Q}\tilde{\mathbf{x}}(t) \frac{d(\tilde{\mathbf{x}}^T(t)\mathbf{P}\tilde{\mathbf{x}}(t))}{d(\tilde{\mathbf{x}}^T(t)\mathbf{P}\tilde{\mathbf{x}}(t))} + \\ & 2\text{tr}\left(\tilde{\mathbf{K}}_x^T(t)\mathbf{x}(t)\tilde{\mathbf{x}}^T(t)\mathbf{PBA} \frac{d(\tilde{\mathbf{x}}^T(t)\mathbf{P}\tilde{\mathbf{x}}(t))}{d(\tilde{\mathbf{x}}^T(t)\mathbf{P}\tilde{\mathbf{x}}(t))} + \right. \\ & \left. \tilde{\mathbf{K}}_x^T(t)\Gamma_x^{-1}\dot{\tilde{\mathbf{K}}}_x(t)\boldsymbol{\Lambda}\right) + \\ & 2\text{tr}\left(\tilde{\mathbf{K}}_r^T(t)\mathbf{r}(t)\tilde{\mathbf{x}}^T(t)\mathbf{PBA} \frac{d(\tilde{\mathbf{x}}^T(t)\mathbf{P}\tilde{\mathbf{x}}(t))}{d(\tilde{\mathbf{x}}^T(t)\mathbf{P}\tilde{\mathbf{x}}(t))} + \right. \\ & \left. \tilde{\mathbf{K}}_r^T(t)\Gamma_r^{-1}\dot{\tilde{\mathbf{K}}}_r(t)\boldsymbol{\Lambda}\right) + \\ & 2\text{tr}\left(\tilde{\boldsymbol{\theta}}^T(t)\boldsymbol{\mu}(\mathbf{x}(t))\tilde{\mathbf{x}}^T(t)\mathbf{PBA} \frac{d(\tilde{\mathbf{x}}^T(t)\mathbf{P}\tilde{\mathbf{x}}(t))}{d(\tilde{\mathbf{x}}^T(t)\mathbf{P}\tilde{\mathbf{x}}(t))} - \right. \\ & \left. \tilde{\boldsymbol{\theta}}^T(t)\Gamma_\theta^{-1}\dot{\tilde{\boldsymbol{\theta}}}(t)\boldsymbol{\Lambda}\right) \end{aligned} \quad (32)$$

Choosing the following MRAC adaptive laws:

$$\begin{aligned} \dot{\tilde{\mathbf{K}}}_x(t) = & \hat{\mathbf{K}}_x(t) - \dot{\mathbf{K}}_x = \hat{\mathbf{K}}_x(t) = \\ & -\Gamma_x\mathbf{x}(t)\tilde{\mathbf{x}}^T(t)\mathbf{PB} \frac{d(\tilde{\mathbf{x}}^T(t)\mathbf{P}\tilde{\mathbf{x}}(t))}{d(\tilde{\mathbf{x}}^T(t)\mathbf{P}\tilde{\mathbf{x}}(t))} \\ \dot{\tilde{\mathbf{K}}}_r(t) = & \hat{\mathbf{K}}_r(t) - \dot{\mathbf{K}}_r = \hat{\mathbf{K}}_r(t) = \\ & -\Gamma_r\mathbf{r}(t)\tilde{\mathbf{x}}^T(t)\mathbf{PB} \frac{d(\tilde{\mathbf{x}}^T(t)\mathbf{P}\tilde{\mathbf{x}}(t))}{d(\tilde{\mathbf{x}}^T(t)\mathbf{P}\tilde{\mathbf{x}}(t))} \end{aligned} \quad (33)$$

$$\begin{aligned} \dot{\tilde{\boldsymbol{\theta}}}(t) = & \hat{\boldsymbol{\theta}}(t) - \dot{\boldsymbol{\theta}} = \hat{\boldsymbol{\theta}}(t) = \\ & \Gamma_\theta\boldsymbol{\mu}(\mathbf{x}(t))\tilde{\mathbf{x}}^T(t)\mathbf{PB} \frac{d(\tilde{\mathbf{x}}^T(t)\mathbf{P}\tilde{\mathbf{x}}(t))}{d(\tilde{\mathbf{x}}^T(t)\mathbf{P}\tilde{\mathbf{x}}(t))} \end{aligned}$$

Yields:

$$\dot{V} = -\tilde{\mathbf{x}}^T(t)\mathbf{Q}\tilde{\mathbf{x}}(t) \frac{d(\tilde{\mathbf{x}}^T(t)\mathbf{P}\tilde{\mathbf{x}}(t))}{d(\tilde{\mathbf{x}}^T(t)\mathbf{P}\tilde{\mathbf{x}}(t))} \leq 0 \quad (34)$$

Equation (34) Proves uniform ultimate boundedness of $\tilde{\mathbf{x}}(t)$, $\tilde{\mathbf{K}}_x(t)$, $\tilde{\mathbf{K}}_r(t)$, $\tilde{\boldsymbol{\theta}}(t)$. Since \mathbf{r} is a bounded command and \mathbf{A}_m is a Hurwitz matrix, then \mathbf{x}_m , is bounded. Using Equation (14) $\mathbf{x} = \tilde{\mathbf{x}} + \mathbf{x}_m$, we can conclude that \mathbf{x} is a bounded signal. We know that the ideal control gains \mathbf{K}_x , \mathbf{K}_r , $\boldsymbol{\theta}$ are constant, therefore using the fact that $\tilde{\mathbf{K}}_x(t)$, $\tilde{\mathbf{K}}_r(t)$, $\tilde{\boldsymbol{\theta}}(t)$ are bounded, then using Equation (22) implies that $\tilde{\mathbf{K}}_x(t)$, $\tilde{\mathbf{K}}_r(t)$, $\tilde{\boldsymbol{\theta}}(t)$ are bounded. Calculating the second time derivative of the Lyapunov function yields:

$$\begin{aligned} \ddot{V} = & -[\tilde{\mathbf{x}}^T(t)(\mathbf{A}_m^T\mathbf{Q} + \mathbf{Q}\mathbf{A}_m)\tilde{\mathbf{x}}(t) + \\ & 2\tilde{\mathbf{x}}^T(t)\mathbf{PBA}\tilde{\mathbf{K}}_x^T(t)\mathbf{x}(t) + 2\tilde{\mathbf{x}}^T(t)\mathbf{PBA}\tilde{\mathbf{K}}_r^T(t)\mathbf{r}(t) - \\ & 2\tilde{\mathbf{x}}^T(t)\mathbf{PBA}\tilde{\boldsymbol{\theta}}^T(t)\boldsymbol{\mu}(\mathbf{x}(t))] \frac{d(\tilde{\mathbf{x}}^T(t)\mathbf{P}\tilde{\mathbf{x}}(t))}{d(\tilde{\mathbf{x}}^T(t)\mathbf{P}\tilde{\mathbf{x}}(t))} - \\ & \tilde{\mathbf{x}}^T(t)\mathbf{Q}\tilde{\mathbf{x}}(t)[\tilde{\mathbf{x}}^T(t)(\mathbf{A}_m^T\mathbf{P} + \mathbf{P}\mathbf{A}_m)\tilde{\mathbf{x}}(t) + \\ & 2\tilde{\mathbf{x}}^T(t)\mathbf{PBA}\tilde{\mathbf{K}}_x^T(t)\mathbf{x}(t) + 2\tilde{\mathbf{x}}^T(t)\mathbf{PBA}\tilde{\mathbf{K}}_r^T(t)\mathbf{r}(t) - \\ & 2\tilde{\mathbf{x}}^T(t)\mathbf{PBA}\tilde{\boldsymbol{\theta}}^T(t)\boldsymbol{\mu}(\mathbf{x}(t))] \frac{d^2(\tilde{\mathbf{x}}^T(t)\mathbf{P}\tilde{\mathbf{x}}(t))}{(d(\tilde{\mathbf{x}}^T(t)\mathbf{P}\tilde{\mathbf{x}}(t)))^2} \end{aligned} \quad (35)$$

We know that every continuously differentiable function ($f \in C^1$) on a compact set is Lipschitz which has a bounded derivative (Appendix A). 1-Lipschitz condition yields 2-Lipschitz which guarantees the boundedness of the second time derivative (Appendix B). we can conclude that the second time derivative of the Lyapunov function is bounded:

$$\ddot{V} < \infty \quad (36)$$

Equations (34) and (36) indicate that \dot{V} is uniformly continuous of time. Since V is lower bounded and $\dot{V} \leq 0$ and \dot{V} is uniformly continuous then using Barbalat's lemma [30], yields:

$$\lim_{t \rightarrow \infty} \dot{V} = \lim_{t \rightarrow \infty} [-\tilde{\mathbf{x}}^T(t)\mathbf{Q}\tilde{\mathbf{x}}(t) \frac{d(\tilde{\mathbf{x}}^T(t)\mathbf{P}\tilde{\mathbf{x}}(t))}{d(\tilde{\mathbf{x}}^T(t)\mathbf{P}\tilde{\mathbf{x}}(t))}] = 0 \quad (37)$$

We know that $\frac{d(\tilde{\mathbf{x}}^T(t)\mathbf{P}\tilde{\mathbf{x}}(t))}{d(\tilde{\mathbf{x}}^T(t)\mathbf{P}\tilde{\mathbf{x}}(t))} > 0$, therefore:

$$\lim_{t \rightarrow \infty} -\tilde{\mathbf{x}}^T(t)\mathbf{Q}\tilde{\mathbf{x}}(t) = \mathbf{0} \rightarrow \lim_{t \rightarrow \infty} \|\mathbf{x}(t) - \mathbf{x}_m(t)\| = 0 \quad (38)$$

We prove that the tracking error globally uniformly asymptotically tends to zero. The general adaptive law Equation (33) can be considered as an simple adaptive law with variable adaptation gains, $\boldsymbol{\Gamma}' = \boldsymbol{\Gamma} \frac{d(\tilde{\mathbf{x}}^T(t)\mathbf{P}\tilde{\mathbf{x}}(t))}{d(\tilde{\mathbf{x}}^T(t)\mathbf{P}\tilde{\mathbf{x}}(t))}$ which yields:

$$\begin{aligned} \dot{\hat{\mathbf{K}}}_x(t) = & -\boldsymbol{\Gamma}'_x\mathbf{x}(t)\tilde{\mathbf{x}}^T(t)\mathbf{PB} \\ \dot{\hat{\mathbf{K}}}_r(t) = & -\boldsymbol{\Gamma}'_r\mathbf{r}(t)\tilde{\mathbf{x}}^T(t)\mathbf{PB} \\ \dot{\hat{\boldsymbol{\theta}}}(t) = & \boldsymbol{\Gamma}'_\theta\boldsymbol{\mu}(\mathbf{x}(t))\tilde{\mathbf{x}}^T(t)\mathbf{PB} \end{aligned} \quad (39)$$

4. ROBUST MRAC SCHEMES

4. 1. σ – Modification We consider a class of MIMO uncertain systems with matched parametric uncertainty subjected to a bounded external disturbance as follows:

$$\dot{\mathbf{x}}(t) = \mathbf{A}\mathbf{x}(t) + \mathbf{B}\mathbf{\Lambda}[\mathbf{u}(t) + \boldsymbol{\theta}^T\boldsymbol{\mu}(\mathbf{x})] + \boldsymbol{\zeta}(t) \quad (40)$$

In Equation (40), $\mathbf{x}(t) \in \mathbf{R}^n$ is the state vector of the system, $\mathbf{A} \in \mathbf{R}^{n \times n}$ is a known matrix, $\mathbf{B} \in \mathbf{R}^{n \times m}$ is a known control matrix we assume that the pair $(\mathbf{A}, \mathbf{B}\mathbf{\Lambda})$ is controllable, $\mathbf{u}(t) \in \mathbf{R}^m$ is the control signal, $\boldsymbol{\theta} \in \mathbf{R}^{p \times m}$ is a matrix of unknown parameters, $\boldsymbol{\mu}(\mathbf{x}) \in \mathbf{R}^p$ is the known regressor vector, which is a continuous Lipschitz function of $\mathbf{x}(t)$, and $\boldsymbol{\zeta}(t) \in \mathbf{R}^n$ is a bounded external disturbance. We consider the following reference model:

$$\dot{\mathbf{x}}_m(t) = \mathbf{A}_m\mathbf{x}_m(t) + \mathbf{B}_m\mathbf{r}(t) \quad (41)$$

In Equation (41), $\mathbf{A}_m \in \mathbf{R}^{n \times n}$ is a known Hurwitz matrix, $\mathbf{B}_m \in \mathbf{R}^{n \times r}$ is assumed to be known, and $\mathbf{r}(t) \in \mathbf{R}^r$ is a bounded time-varying reference command.

Assumption: given matrices \mathbf{A} and \mathbf{B} , there exist matrices \mathbf{K}_x and \mathbf{K}_r such that Equation (42) be satisfied.

$$\begin{aligned} \mathbf{A}_m &= \mathbf{A} + \mathbf{B}\mathbf{\Lambda}\mathbf{K}_x^T \\ \mathbf{B}_m &= \mathbf{B}\mathbf{\Lambda}\mathbf{K}_r^T \end{aligned} \quad (42)$$

We use the control input $\mathbf{u}(t)$ as follows:

$$\mathbf{u} = \mathbf{K}_x\mathbf{x} + \mathbf{K}_r\mathbf{r} - \tilde{\boldsymbol{\theta}}^T\boldsymbol{\mu}(\mathbf{x}) \quad (43)$$

Subtracting Equation (41) from Equation (40) yields:

$$\begin{aligned} \dot{\mathbf{x}}(t) - \dot{\mathbf{x}}_m(t) &= \mathbf{A}\mathbf{x}(t) + \mathbf{B}\mathbf{\Lambda}[\mathbf{u}(t) + \boldsymbol{\theta}^T\boldsymbol{\mu}(\mathbf{x})] + \\ \boldsymbol{\zeta}(t) - \mathbf{A}_m\mathbf{x}_m(t) - \mathbf{B}_m\mathbf{r}(t) \end{aligned} \quad (44)$$

Substituting Equation (43) in Equation (44) and using Equation (42) gives:

$$\begin{aligned} \dot{\mathbf{x}}(t) - \dot{\mathbf{x}}_m(t) &= \mathbf{A}_m\mathbf{x}(t) - \mathbf{B}\mathbf{\Lambda}(\tilde{\boldsymbol{\theta}}^T - \boldsymbol{\theta}^T)\boldsymbol{\mu}(\mathbf{x}) + \\ \boldsymbol{\zeta}(t) - \mathbf{A}_m\mathbf{x}_m(t) \end{aligned} \quad (45)$$

Simplifying Equation (45) yields the tracking error dynamics:

$$\dot{\tilde{\mathbf{x}}} = \mathbf{A}_m\tilde{\mathbf{x}} - \mathbf{B}\mathbf{\Lambda}\tilde{\boldsymbol{\theta}}^T\boldsymbol{\mu}(\mathbf{x}) + \boldsymbol{\zeta}(t) \quad (46)$$

The σ – Modification to the MRAC adaptive law is:

$$\dot{\tilde{\boldsymbol{\theta}}} = \Gamma(\boldsymbol{\mu}(\mathbf{x})\tilde{\mathbf{x}}^T\mathbf{P}\mathbf{B} \frac{df(\tilde{\mathbf{x}}^T(t)\mathbf{P}\tilde{\mathbf{x}}(t))}{d(\tilde{\mathbf{x}}^T(t)\mathbf{P}\tilde{\mathbf{x}}(t))} - \sigma\tilde{\boldsymbol{\theta}}) \quad (47)$$

In Equation (47), $\sigma > 0$ is the modification parameter. Now we consider the following radially unbounded Lyapunov function candidate:

$$V(\tilde{\mathbf{x}}, \tilde{\boldsymbol{\theta}}) = f(\tilde{\mathbf{x}}^T(t)\mathbf{P}\tilde{\mathbf{x}}(t)) + \text{tr}(\tilde{\boldsymbol{\theta}}^T\Gamma^{-1}\tilde{\boldsymbol{\theta}}\mathbf{\Lambda}) \quad (48)$$

The first time derivative of the Lyapunov function candidates becomes:

$$\begin{aligned} \dot{V}(\tilde{\mathbf{x}}, \tilde{\boldsymbol{\theta}}) &= (\dot{\tilde{\mathbf{x}}}^T\mathbf{P}\tilde{\mathbf{x}} + \tilde{\mathbf{x}}^T\mathbf{P}\dot{\tilde{\mathbf{x}}}) \frac{df(\tilde{\mathbf{x}}^T(t)\mathbf{P}\tilde{\mathbf{x}}(t))}{d(\tilde{\mathbf{x}}^T(t)\mathbf{P}\tilde{\mathbf{x}}(t))} + \\ &2\text{tr}(\tilde{\boldsymbol{\theta}}^T\Gamma^{-1}\dot{\tilde{\boldsymbol{\theta}}}\mathbf{\Lambda}) \end{aligned} \quad (49)$$

Using Equations (46) and (49) yields:

$$\begin{aligned} \dot{V}(\tilde{\mathbf{x}}, \tilde{\boldsymbol{\theta}}) &= [(\tilde{\mathbf{x}}^T\mathbf{A}_m^T - \boldsymbol{\mu}^T(\mathbf{x})\tilde{\boldsymbol{\theta}}\mathbf{\Lambda}\mathbf{B}^T + \boldsymbol{\zeta}^T)\mathbf{P}\tilde{\mathbf{x}} + \\ \tilde{\mathbf{x}}^T\mathbf{P}(\mathbf{A}_m\tilde{\mathbf{x}} - \mathbf{B}\mathbf{\Lambda}\tilde{\boldsymbol{\theta}}^T\boldsymbol{\mu}(\mathbf{x}) + \boldsymbol{\zeta})] \frac{df(\tilde{\mathbf{x}}^T(t)\mathbf{P}\tilde{\mathbf{x}}(t))}{d(\tilde{\mathbf{x}}^T(t)\mathbf{P}\tilde{\mathbf{x}}(t))} + \\ &2\text{tr}[\tilde{\boldsymbol{\theta}}^T\Gamma^{-1}(\Gamma[(\boldsymbol{\mu}(\mathbf{x})\tilde{\mathbf{x}}^T\mathbf{P}\mathbf{B} \frac{df(\tilde{\mathbf{x}}^T(t)\mathbf{P}\tilde{\mathbf{x}}(t))}{d(\tilde{\mathbf{x}}^T(t)\mathbf{P}\tilde{\mathbf{x}}(t))} - \sigma\tilde{\boldsymbol{\theta}})])\mathbf{\Lambda}] \end{aligned} \quad (50)$$

Simplifying Equation (50) yields:

$$\begin{aligned} \dot{V}(\tilde{\mathbf{x}}, \tilde{\boldsymbol{\theta}}) &= \tilde{\mathbf{x}}^T[\mathbf{A}_m^T\mathbf{P} + \mathbf{P}\mathbf{A}_m]\tilde{\mathbf{x}} \frac{df(\tilde{\mathbf{x}}^T(t)\mathbf{P}\tilde{\mathbf{x}}(t))}{d(\tilde{\mathbf{x}}^T(t)\mathbf{P}\tilde{\mathbf{x}}(t))} + \\ &2\tilde{\mathbf{x}}^T\mathbf{P}\boldsymbol{\zeta} \frac{df(\tilde{\mathbf{x}}^T(t)\mathbf{P}\tilde{\mathbf{x}}(t))}{d(\tilde{\mathbf{x}}^T(t)\mathbf{P}\tilde{\mathbf{x}}(t))} \\ &- 2\tilde{\mathbf{x}}^T\mathbf{P}\mathbf{B}\mathbf{\Lambda}\tilde{\boldsymbol{\theta}}^T\boldsymbol{\mu}(\mathbf{x}) \frac{df(\tilde{\mathbf{x}}^T(t)\mathbf{P}\tilde{\mathbf{x}}(t))}{d(\tilde{\mathbf{x}}^T(t)\mathbf{P}\tilde{\mathbf{x}}(t))} + \\ &2\text{tr}[\tilde{\boldsymbol{\theta}}^T\boldsymbol{\mu}(\mathbf{x})\tilde{\mathbf{x}}^T\mathbf{P}\mathbf{B}\mathbf{\Lambda} \frac{df(\tilde{\mathbf{x}}^T(t)\mathbf{P}\tilde{\mathbf{x}}(t))}{d(\tilde{\mathbf{x}}^T(t)\mathbf{P}\tilde{\mathbf{x}}(t))} - \sigma\tilde{\boldsymbol{\theta}}^T\tilde{\boldsymbol{\theta}}\mathbf{\Lambda}] \end{aligned} \quad (51)$$

Using the vector- trace identity Equation (30) and the algebraic Lyapunov equation:

$$\mathbf{A}_m^T\mathbf{P} + \mathbf{P}\mathbf{A}_m = -\mathbf{Q} \quad (52)$$

Equation (51) becomes:

$$\begin{aligned} \dot{V}(\tilde{\mathbf{x}}, \tilde{\boldsymbol{\theta}}) &= (-\tilde{\mathbf{x}}^T\mathbf{Q}\tilde{\mathbf{x}} + 2\tilde{\mathbf{x}}^T\mathbf{P}\boldsymbol{\zeta}) \frac{df(\tilde{\mathbf{x}}^T(t)\mathbf{P}\tilde{\mathbf{x}}(t))}{d(\tilde{\mathbf{x}}^T(t)\mathbf{P}\tilde{\mathbf{x}}(t))} - \\ &2\sigma\text{tr}[\tilde{\boldsymbol{\theta}}^T\tilde{\boldsymbol{\theta}}\mathbf{\Lambda}] \end{aligned} \quad (53)$$

Using:

$$\tilde{\boldsymbol{\theta}} = \tilde{\boldsymbol{\theta}} + \boldsymbol{\theta} \quad (54)$$

Yields:

$$\begin{aligned} \dot{V}(\tilde{\mathbf{x}}, \tilde{\boldsymbol{\theta}}) &= (-\tilde{\mathbf{x}}^T\mathbf{Q}\tilde{\mathbf{x}} + 2\tilde{\mathbf{x}}^T\mathbf{P}\boldsymbol{\zeta}) \frac{df(\tilde{\mathbf{x}}^T(t)\mathbf{P}\tilde{\mathbf{x}}(t))}{d(\tilde{\mathbf{x}}^T(t)\mathbf{P}\tilde{\mathbf{x}}(t))} - \\ &2\sigma\text{tr}[\tilde{\boldsymbol{\theta}}^T\tilde{\boldsymbol{\theta}}\mathbf{\Lambda}] - 2\sigma\text{tr}[\tilde{\boldsymbol{\theta}}^T\boldsymbol{\theta}\mathbf{\Lambda}] \end{aligned} \quad (55)$$

We use the Frobenius norm definition, and the Cauchy Schwarz inequality (51) presented as follows:

$$\text{tr}[\tilde{\boldsymbol{\theta}}^T\tilde{\boldsymbol{\theta}}\mathbf{\Lambda}] = \sum_{i=1}^n \sum_{j=1}^m \tilde{\theta}_{ij}^2 \Lambda_{ii} \geq \|\tilde{\boldsymbol{\theta}}\|_F^2 \Lambda_{\min} \quad (56)$$

$$|\text{tr}(\tilde{\boldsymbol{\theta}}^T\boldsymbol{\theta}\mathbf{\Lambda})| \leq \|\tilde{\boldsymbol{\theta}}^T\boldsymbol{\theta}\|_F \|\mathbf{\Lambda}\|_F \leq \|\tilde{\boldsymbol{\theta}}\|_F \|\boldsymbol{\theta}\|_F \|\mathbf{\Lambda}\|_F$$

The upper bound of the external disturbance and unknown parameters are considered as follows:

$$\zeta_0 = \max\|\boldsymbol{\zeta}\|_\infty \quad (57)$$

$$\theta_0 = \|\boldsymbol{\theta}\|_F$$

Using Equations (56), and (57), Equation (55) can be written as follows:

$$\begin{aligned} \dot{V}(\tilde{\mathbf{x}}, \tilde{\boldsymbol{\theta}}) &\leq [-\lambda_{\min}(\mathbf{Q})\|\tilde{\mathbf{x}}\|^2 + \\ &2\|\tilde{\mathbf{x}}\|\lambda_{\max}(\mathbf{P})\zeta_0] \frac{df(\tilde{\mathbf{x}}^T(t)\mathbf{P}\tilde{\mathbf{x}}(t))}{d(\tilde{\mathbf{x}}^T(t)\mathbf{P}\tilde{\mathbf{x}}(t))} - 2\sigma\|\tilde{\boldsymbol{\theta}}\|_F^2 \Lambda_{\min} + \\ &2\sigma\|\tilde{\boldsymbol{\theta}}\|_F \|\boldsymbol{\theta}\|_F \|\mathbf{\Lambda}\|_F \end{aligned} \quad (58)$$

We use the following inequality:

$$2ab \leq a^2 + b^2 \quad (59)$$

Equation (58) becomes:

$$\begin{aligned}
\dot{V}(\tilde{\mathbf{x}}, \tilde{\boldsymbol{\theta}}) &\leq (-\lambda_{\min}(\mathbf{Q})\|\tilde{\mathbf{x}}\|^2 + \\
&2\|\tilde{\mathbf{x}}\|\lambda_{\max}(\mathbf{P})\zeta_0) \frac{df(\tilde{\mathbf{x}}^T(t)\mathbf{P}\tilde{\mathbf{x}}(t))}{d(\tilde{\mathbf{x}}^T(t)\mathbf{P}\tilde{\mathbf{x}}(t))} - 2\sigma\|\tilde{\boldsymbol{\theta}}\|_F^2\Lambda_{\min} + \\
&\sigma(\|\tilde{\boldsymbol{\theta}}\|_F^2 + \|\boldsymbol{\theta}\|_F^2)\|\Lambda\|_F \\
&= (-\lambda_{\min}(\mathbf{Q})\|\tilde{\mathbf{x}}\|^2 + \\
&2\|\tilde{\mathbf{x}}\|\lambda_{\max}(\mathbf{P})\zeta_0) \frac{df(\tilde{\mathbf{x}}^T(t)\mathbf{P}\tilde{\mathbf{x}}(t))}{d(\tilde{\mathbf{x}}^T(t)\mathbf{P}\tilde{\mathbf{x}}(t))} - \sigma\|\tilde{\boldsymbol{\theta}}\|_F^2(2\Lambda_{\min} + \\
&\|\Lambda\|_F) + \sigma\|\boldsymbol{\theta}\|_F^2\|\Lambda\|_F
\end{aligned} \quad (60)$$

If we choose:

$$\begin{aligned}
-\lambda_{\min}(\mathbf{Q})\|\tilde{\mathbf{x}}\|^2 + 2\|\tilde{\mathbf{x}}\|\lambda_{\max}(\mathbf{P})\zeta_0 &\leq 0 \\
-\sigma\|\tilde{\boldsymbol{\theta}}\|_F^2(2\Lambda_{\min} + \|\Lambda\|_F) + \sigma\|\boldsymbol{\theta}\|_F^2\|\Lambda\|_F &\leq 0
\end{aligned} \quad (61)$$

Or:

$$\begin{aligned}
\Omega = \{(\tilde{\mathbf{x}}, \tilde{\boldsymbol{\theta}}): \|\tilde{\mathbf{x}}\| < \frac{2\lambda_{\max}(\mathbf{P})\zeta_0}{\lambda_{\min}(\mathbf{Q})} \wedge \|\tilde{\boldsymbol{\theta}}\|_F \leq \\
\sqrt{\frac{\|\boldsymbol{\theta}\|_F^2\|\Lambda\|_F}{2\Lambda_{\min} + \|\Lambda\|_F}}\}
\end{aligned} \quad (62)$$

Then we have $\dot{V} \leq 0$ outside of the compact set Ω , and $\dot{V} > 0$ inside it. We prove that all signals in the closed-loop system are uniformly, ultimately bounded.

4. 2. e-Modification By definition, the e-Modification to the MRAC adaptive law that estimates $\tilde{\boldsymbol{\theta}}(t)$ is:

$$\dot{\tilde{\boldsymbol{\theta}}} = \Gamma \frac{df(\tilde{\mathbf{x}}^T(t)\mathbf{P}\tilde{\mathbf{x}}(t))}{d(\tilde{\mathbf{x}}^T(t)\mathbf{P}\tilde{\mathbf{x}}(t))} (\boldsymbol{\mu}(\mathbf{x})\tilde{\mathbf{x}}^T\mathbf{P}\mathbf{B} - \alpha\|\tilde{\mathbf{x}}^T\mathbf{P}\mathbf{B}\|\tilde{\boldsymbol{\theta}}) \quad (63)$$

In Equation (63), $\alpha > 0$ is the modification parameter. We consider the following radially unbounded Lyapunov function:

$$V(\tilde{\mathbf{x}}, \tilde{\boldsymbol{\theta}}) = f(\tilde{\mathbf{x}}^T(t)\mathbf{P}\tilde{\mathbf{x}}(t)) + \text{tr}(\tilde{\boldsymbol{\theta}}^T\Gamma^{-1}\tilde{\boldsymbol{\theta}}\Lambda) \quad (64)$$

The first time derivative of the Equation (64) becomes:

$$\begin{aligned}
\dot{V}(\tilde{\mathbf{x}}, \tilde{\boldsymbol{\theta}}) &= (\dot{\tilde{\mathbf{x}}}^T\mathbf{P}\tilde{\mathbf{x}} + \tilde{\mathbf{x}}^T\mathbf{P}\dot{\tilde{\mathbf{x}}}) \frac{df(\tilde{\mathbf{x}}^T(t)\mathbf{P}\tilde{\mathbf{x}}(t))}{d(\tilde{\mathbf{x}}^T(t)\mathbf{P}\tilde{\mathbf{x}}(t))} + \\
&2\text{tr}(\tilde{\boldsymbol{\theta}}^T\Gamma^{-1}\dot{\tilde{\boldsymbol{\theta}}}\Lambda)
\end{aligned} \quad (65)$$

Using the tracking error dynamics Equation (46) yields:

$$\begin{aligned}
\dot{V}(\tilde{\mathbf{x}}, \tilde{\boldsymbol{\theta}}) &= [(\tilde{\mathbf{x}}^T\mathbf{A}_m^T - \boldsymbol{\mu}^T(\mathbf{x})\tilde{\boldsymbol{\theta}}\Lambda\mathbf{B}^T + \boldsymbol{\zeta}^T)\mathbf{P}\tilde{\mathbf{x}} + \\
&\tilde{\mathbf{x}}^T\mathbf{P}(\mathbf{A}_m\tilde{\mathbf{x}} - \mathbf{B}\Lambda\tilde{\boldsymbol{\theta}}^T\boldsymbol{\mu}(\mathbf{x}) + \boldsymbol{\zeta})] \frac{df(\tilde{\mathbf{x}}^T(t)\mathbf{P}\tilde{\mathbf{x}}(t))}{d(\tilde{\mathbf{x}}^T(t)\mathbf{P}\tilde{\mathbf{x}}(t))} + \\
&2\text{tr}(\tilde{\boldsymbol{\theta}}^T\Gamma^{-1} \left(\Gamma \frac{df(\tilde{\mathbf{x}}^T(t)\mathbf{P}\tilde{\mathbf{x}}(t))}{d(\tilde{\mathbf{x}}^T(t)\mathbf{P}\tilde{\mathbf{x}}(t))} (\boldsymbol{\mu}(\mathbf{x})\tilde{\mathbf{x}}^T\mathbf{P}\mathbf{B} - \right. \\
&\left. \alpha\|\tilde{\mathbf{x}}^T\mathbf{P}\mathbf{B}\|\tilde{\boldsymbol{\theta}}\Lambda) \right)
\end{aligned} \quad (66)$$

Simplifying Equation (66) gives:

$$\begin{aligned}
\dot{V}(\tilde{\mathbf{x}}, \tilde{\boldsymbol{\theta}}) &= \tilde{\mathbf{x}}^T[\mathbf{A}_m^T\mathbf{P} + \mathbf{P}\mathbf{A}_m]\tilde{\mathbf{x}} \frac{df(\tilde{\mathbf{x}}^T(t)\mathbf{P}\tilde{\mathbf{x}}(t))}{d(\tilde{\mathbf{x}}^T(t)\mathbf{P}\tilde{\mathbf{x}}(t))} + \\
&2\tilde{\mathbf{x}}^T\mathbf{P}\boldsymbol{\zeta} \frac{df(\tilde{\mathbf{x}}^T(t)\mathbf{P}\tilde{\mathbf{x}}(t))}{d(\tilde{\mathbf{x}}^T(t)\mathbf{P}\tilde{\mathbf{x}}(t))} - \\
&2\tilde{\mathbf{x}}^T\mathbf{P}\mathbf{B}\Lambda\tilde{\boldsymbol{\theta}}^T\boldsymbol{\mu}(\mathbf{x}) \frac{df(\tilde{\mathbf{x}}^T(t)\mathbf{P}\tilde{\mathbf{x}}(t))}{d(\tilde{\mathbf{x}}^T(t)\mathbf{P}\tilde{\mathbf{x}}(t))} + \\
&2 \frac{df(\tilde{\mathbf{x}}^T(t)\mathbf{P}\tilde{\mathbf{x}}(t))}{d(\tilde{\mathbf{x}}^T(t)\mathbf{P}\tilde{\mathbf{x}}(t))} \text{tr}[(\tilde{\boldsymbol{\theta}}^T\boldsymbol{\mu}(\mathbf{x})\tilde{\mathbf{x}}^T\mathbf{P}\mathbf{B} - \alpha\|\tilde{\mathbf{x}}^T\mathbf{P}\mathbf{B}\|\tilde{\boldsymbol{\theta}})\Lambda]
\end{aligned} \quad (67)$$

Same as the previous section using the vector- trace identity Equation (30) and the algebraic Lyapunov Equation (52) yields:

$$\begin{aligned}
\dot{V}(\tilde{\mathbf{x}}, \tilde{\boldsymbol{\theta}}) &= (-\tilde{\mathbf{x}}^T\mathbf{Q}\tilde{\mathbf{x}} + 2\tilde{\mathbf{x}}^T\mathbf{P}\boldsymbol{\zeta}) \frac{df(\tilde{\mathbf{x}}^T(t)\mathbf{P}\tilde{\mathbf{x}}(t))}{d(\tilde{\mathbf{x}}^T(t)\mathbf{P}\tilde{\mathbf{x}}(t))} - \\
&2\alpha\|\tilde{\mathbf{x}}^T\mathbf{P}\mathbf{B}\|\text{tr}[\tilde{\boldsymbol{\theta}}^T\tilde{\boldsymbol{\theta}}\Lambda]
\end{aligned} \quad (68)$$

Using $\tilde{\boldsymbol{\theta}} = \tilde{\boldsymbol{\theta}} + \boldsymbol{\theta}$:

$$\begin{aligned}
\dot{V}(\tilde{\mathbf{x}}, \tilde{\boldsymbol{\theta}}) &= (-\tilde{\mathbf{x}}^T\mathbf{Q}\tilde{\mathbf{x}} + 2\tilde{\mathbf{x}}^T\mathbf{P}\boldsymbol{\zeta}) \frac{df(\tilde{\mathbf{x}}^T(t)\mathbf{P}\tilde{\mathbf{x}}(t))}{d(\tilde{\mathbf{x}}^T(t)\mathbf{P}\tilde{\mathbf{x}}(t))} - \\
&2\alpha\|\tilde{\mathbf{x}}^T\mathbf{P}\mathbf{B}\|\text{tr}[\tilde{\boldsymbol{\theta}}^T\tilde{\boldsymbol{\theta}}\Lambda] - 2\alpha\|\tilde{\mathbf{x}}^T\mathbf{P}\mathbf{B}\|\text{tr}[\tilde{\boldsymbol{\theta}}^T\boldsymbol{\theta}\Lambda]
\end{aligned} \quad (69)$$

Using the Frobenius norm and the Cauchy Schwartz inequality (56) and the upper bound of the external disturbance and unknown parameters Equation (57), we have the following inequality:

$$\begin{aligned}
\dot{V}(\tilde{\mathbf{x}}, \tilde{\boldsymbol{\theta}}) &\leq \\
&[-\lambda_{\min}(\mathbf{Q})\|\tilde{\mathbf{x}}\|^2 + 2\|\tilde{\mathbf{x}}\|\lambda_{\max}(\mathbf{P})\zeta_0] \frac{df(\tilde{\mathbf{x}}^T(t)\mathbf{P}\tilde{\mathbf{x}}(t))}{d(\tilde{\mathbf{x}}^T(t)\mathbf{P}\tilde{\mathbf{x}}(t))} - \\
&2\alpha\|\tilde{\mathbf{x}}^T\mathbf{P}\mathbf{B}\|\|\tilde{\boldsymbol{\theta}}\|_F^2\Lambda_{\min} + 2\alpha\|\tilde{\mathbf{x}}^T\mathbf{P}\mathbf{B}\|\|\tilde{\boldsymbol{\theta}}\|_F\|\boldsymbol{\theta}\|_F\|\Lambda\|_F
\end{aligned} \quad (70)$$

Using Equation (59) gives:

$$\begin{aligned}
\dot{V}(\tilde{\mathbf{x}}, \tilde{\boldsymbol{\theta}}) &\leq (-\lambda_{\min}(\mathbf{Q})\|\tilde{\mathbf{x}}\|^2 + \\
&2\|\tilde{\mathbf{x}}\|\lambda_{\max}(\mathbf{P})\zeta_0) \frac{df(\tilde{\mathbf{x}}^T(t)\mathbf{P}\tilde{\mathbf{x}}(t))}{d(\tilde{\mathbf{x}}^T(t)\mathbf{P}\tilde{\mathbf{x}}(t))} - \\
&2\alpha\|\tilde{\mathbf{x}}^T\mathbf{P}\mathbf{B}\|\|\tilde{\boldsymbol{\theta}}\|_F^2\Lambda_{\min} + \alpha\|\tilde{\mathbf{x}}^T\mathbf{P}\mathbf{B}\|(\|\tilde{\boldsymbol{\theta}}\|_F^2 + \\
&\|\boldsymbol{\theta}\|_F^2)\|\Lambda\|_F = (-\lambda_{\min}(\mathbf{Q})\|\tilde{\mathbf{x}}\|^2 + \\
&2\|\tilde{\mathbf{x}}\|\lambda_{\max}(\mathbf{P})\zeta_0) \frac{df(\tilde{\mathbf{x}}^T(t)\mathbf{P}\tilde{\mathbf{x}}(t))}{d(\tilde{\mathbf{x}}^T(t)\mathbf{P}\tilde{\mathbf{x}}(t))} - \\
&\alpha\|\tilde{\mathbf{x}}^T\mathbf{P}\mathbf{B}\|\|\tilde{\boldsymbol{\theta}}\|_F^2(2\Lambda_{\min} + \|\Lambda\|_F) + \\
&\alpha\|\tilde{\mathbf{x}}^T\mathbf{P}\mathbf{B}\|\|\boldsymbol{\theta}\|_F^2\|\Lambda\|_F
\end{aligned} \quad (71)$$

If we choose:

$$\begin{aligned}
-\lambda_{\min}(\mathbf{Q})\|\tilde{\mathbf{x}}\|^2 + 2\|\tilde{\mathbf{x}}\|\lambda_{\max}(\mathbf{P})\zeta_0 &\leq 0 \\
-\alpha\|\tilde{\mathbf{x}}^T\mathbf{P}\mathbf{B}\|\|\tilde{\boldsymbol{\theta}}\|_F^2(2\Lambda_{\min} + \|\Lambda\|_F) + \\
\alpha\|\tilde{\mathbf{x}}^T\mathbf{P}\mathbf{B}\|\|\boldsymbol{\theta}\|_F^2\|\Lambda\|_F &\leq 0
\end{aligned} \quad (72)$$

Or:

$$\begin{aligned}
\Omega = \{(\tilde{\mathbf{x}}, \tilde{\boldsymbol{\theta}}): \|\tilde{\mathbf{x}}\| < \frac{2\lambda_{\max}(\mathbf{P})\zeta_0}{\lambda_{\min}(\mathbf{Q})} \wedge \|\tilde{\boldsymbol{\theta}}\|_F \leq \\
\sqrt{\frac{\|\boldsymbol{\theta}\|_F^2\|\Lambda\|_F}{2\Lambda_{\min} + \|\Lambda\|_F}}\}
\end{aligned} \quad (73)$$

Same as the previous section, we have $\dot{V} \leq 0$ outside of the compact set Ω , and $\dot{V} > 0$ inside it, and all signals in the closed-loop system are uniformly ultimately bounded.

5. SIMULATIONS

5. 1. MRAC Scheme In this section, the validity of the proposed general MRAC adaptive law is verified by considering an arbitrary Lyapunov function candidate. The value of the control effectiveness (uncertainty) is chosen as:

$$d_0 = 1 \tag{74}$$

Considering The following initial conditions for the system states:

$$\begin{aligned} \phi_0 = 5 \text{ deg} \cdot P_0 = 0 \left(\frac{\text{deg}}{\text{s}}\right); \phi_0 = 3.75 \text{ deg} \cdot P_0 = \\ 0 \left(\frac{\text{deg}}{\text{s}}\right); \phi_0 = -3.75 \text{ deg} \cdot P_0 = 0 \left(\frac{\text{deg}}{\text{s}}\right); \phi_0 = \\ -5 \text{ deg} \cdot P_0 = 0 \left(\frac{\text{deg}}{\text{s}}\right) \end{aligned} \tag{75}$$

The reference roll dynamics can be considered in the state-space form:

$$\begin{bmatrix} \dot{\Phi}_m \\ \dot{P}_m \end{bmatrix} = \begin{bmatrix} 0 & 1 \\ -\omega_n^2 & -2\beta\omega_n \end{bmatrix} \begin{bmatrix} \Phi_m \\ P_m \end{bmatrix} + \begin{bmatrix} 0 \\ \omega_n^2 \end{bmatrix} r(t) \tag{76}$$

We use the following parameters for damping and natural frequency and adaptation gains:

$$\begin{aligned} \omega_n = -1. \quad \beta = 0.7 \\ \Gamma_r = 1. \quad \Gamma_x = \begin{bmatrix} 1 & 0 \\ 0 & 1 \end{bmatrix}. \quad \Gamma_\theta = \begin{bmatrix} 1 & 0 & 0 \\ 0 & 1 & 0 \\ 0 & 0 & 1 \end{bmatrix} \end{aligned} \tag{77}$$

Considering the scalar function:

$$f(u) = (1 + u)^{(1+u)^2} - 1 \quad u \geq 0 \tag{78}$$

The first derivative of this function becomes:

$$f'(u) = (1 + u)^{(1+u)^2} [(u + 1) + 2(u + 1)\text{Ln}(u + 1)] \tag{79}$$

It is clear that:

$$f(0) = 0 \text{ and } \forall u \geq 0. f'(u) > 0 \tag{80}$$

Given the fact that every quadratic term is equal or greater than zero, we use the following Lyapunov function candidate:

$$\begin{aligned} V = (1 + \tilde{x}^T(t)P\tilde{x}(t))^{(1+\tilde{x}^T(t)P\tilde{x}(t))^2} - 1 + \\ \text{tr}([\tilde{K}_x^T(t)\Gamma_x^{-1}\tilde{K}_x(t) + \tilde{K}_r^T(t)\Gamma_r^{-1}\tilde{K}_r(t) + \\ \tilde{\theta}^T(t)\Gamma_\theta^{-1}\tilde{\theta}(t)]\Lambda) \end{aligned} \tag{81}$$

According to Equation (33), we have the following adaptive laws:

$$\begin{aligned} \dot{\tilde{K}}_x(t) = -\Gamma_x \tilde{x}(t) \tilde{x}^T(t) P B \left[(1 + \tilde{x}^T(t) P \tilde{x}(t))^{(1+\tilde{x}^T(t) P \tilde{x}(t))^2} \times (1 + \tilde{x}^T(t) P \tilde{x}(t)) \left(1 + 2 \text{Ln} (1 + \tilde{x}^T(t) P \tilde{x}(t)) \right) \right] \\ \dot{\tilde{K}}_r(t) = -\Gamma_r r(t) \tilde{x}^T(t) P B \left[(1 + \tilde{x}^T(t) P \tilde{x}(t))^{(1+\tilde{x}^T(t) P \tilde{x}(t))^2} \times (1 + \tilde{x}^T(t) P \tilde{x}(t)) \left(1 + 2 \text{Ln} (1 + \tilde{x}^T(t) P \tilde{x}(t)) \right) \right] \end{aligned} \tag{82}$$

$$\begin{aligned} \dot{\tilde{\theta}}(t) = \Gamma_\theta \mu(\tilde{x}(t)) \tilde{x}^T(t) P B \left[(1 + \tilde{x}^T(t) P \tilde{x}(t))^{(1+\tilde{x}^T(t) P \tilde{x}(t))^2} \times (1 + \tilde{x}^T(t) P \tilde{x}(t)) \left(1 + 2 \text{Ln} (1 + \tilde{x}^T(t) P \tilde{x}(t)) \right) \right] \end{aligned}$$

Simulation results presented in Figures 5 to 8:

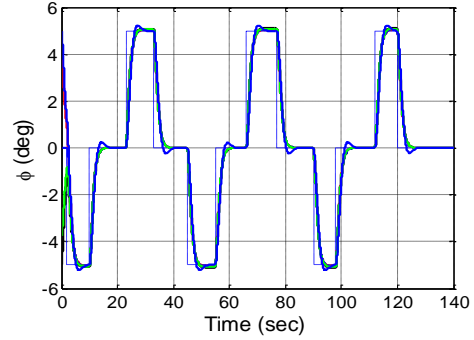


Figure 5. Roll Angle Tracking Performance

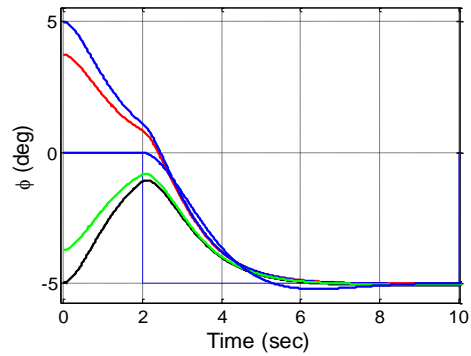


Figure 6. Zoomed Plot from Fig.1 (different initial conditions)

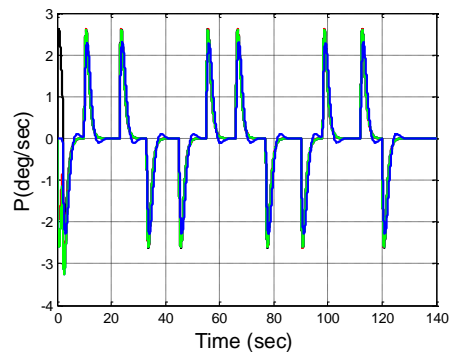


Figure 7. Roll Rate Tracking Performance

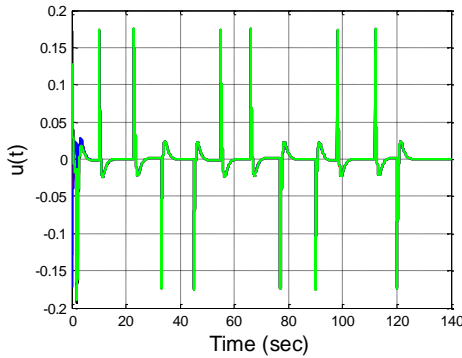


Figure 8. Control Signal (Maximum deflection (20 deg))

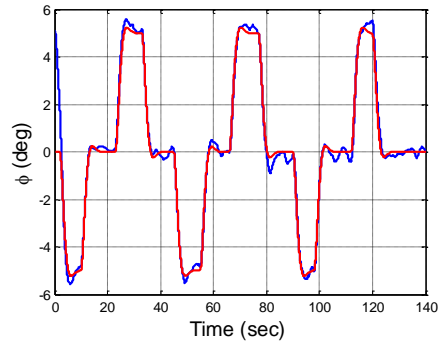


Figure 9. Roll Rate Tracking (σ -modification)

5. 2. Robust Mrac Schemes In this section, the performance of the robust MRAC controllers with general adaptive law by considering an arbitrary Lyapunov function is evaluated. We use the values of the parameters corresponding to $\alpha = 22.5$ deg (Table 1) and considering the following matrices \mathbf{Q} , $\mathbf{\Gamma}$ and modification parameter as follows:

$$\mathbf{Q} = \begin{bmatrix} 1 & 0 \\ 0 & 1 \end{bmatrix}, \mathbf{\Gamma} = \begin{bmatrix} 100 & 0 & 0 \\ 0 & 100 & 0 \\ 0 & 0 & 100 \end{bmatrix} \quad (83)$$

$$\sigma = 0.01, \alpha = 0.01$$

The external disturbance $\zeta(t)$ is modeled as a random process noise, uniformly distributed on the interval $\frac{\pi}{180}[-2 \ 2]$. We consider the following radially unbounded Lyapunov function as follows:

$$V(\tilde{\mathbf{x}}, \tilde{\boldsymbol{\theta}}) = (1 + \tilde{\mathbf{x}}^T(t)\mathbf{P}\tilde{\mathbf{x}}(t))^{(1+\tilde{\mathbf{x}}^T(t)\mathbf{P}\tilde{\mathbf{x}}(t))^2} - 1 + \text{tr}(\tilde{\boldsymbol{\theta}}^T\mathbf{\Gamma}^{-1}\tilde{\boldsymbol{\theta}}\boldsymbol{\Lambda}) \quad (84)$$

Consequently, from Equation (47), we have the following adaptation law for σ – modification scheme:

$$\begin{aligned} \dot{\tilde{\boldsymbol{\theta}}} = & \mathbf{\Gamma}(\boldsymbol{\mu}(\mathbf{x})\tilde{\mathbf{x}}^T\mathbf{P}\mathbf{B}\left(1 + \right. \\ & \left. \tilde{\mathbf{x}}^T(t)\mathbf{P}\tilde{\mathbf{x}}(t)\right)^{(1+\tilde{\mathbf{x}}^T(t)\mathbf{P}\tilde{\mathbf{x}}(t))^2} \left(1 + \tilde{\mathbf{x}}^T(t)\mathbf{P}\tilde{\mathbf{x}}(t)\right) \left(1 + \right. \\ & \left. 2\text{Ln}\left(1 + \tilde{\mathbf{x}}^T(t)\mathbf{P}\tilde{\mathbf{x}}(t)\right)\right) - \sigma\tilde{\boldsymbol{\theta}}) \end{aligned} \quad (85)$$

According to Equation (63), we have the following adaptation law for e – modification:

$$\begin{aligned} \dot{\tilde{\boldsymbol{\theta}}} = & \mathbf{\Gamma} \left(1 + \tilde{\mathbf{x}}^T(t)\mathbf{P}\tilde{\mathbf{x}}(t)\right)^{(1+\tilde{\mathbf{x}}^T(t)\mathbf{P}\tilde{\mathbf{x}}(t))^2} \left(1 + \right. \\ & \left. \tilde{\mathbf{x}}^T(t)\mathbf{P}\tilde{\mathbf{x}}(t)\right) \left(1 + 2\text{Ln}\left(1 + \right. \right. \\ & \left. \left. \tilde{\mathbf{x}}^T(t)\mathbf{P}\tilde{\mathbf{x}}(t)\right)\right) (\boldsymbol{\mu}(\mathbf{x})\tilde{\mathbf{x}}^T\mathbf{P}\mathbf{B} - \alpha\|\tilde{\mathbf{x}}^T\mathbf{P}\mathbf{B}\|\tilde{\boldsymbol{\theta}}) \end{aligned} \quad (86)$$

Simulation results presented in Figures 9 to 16:

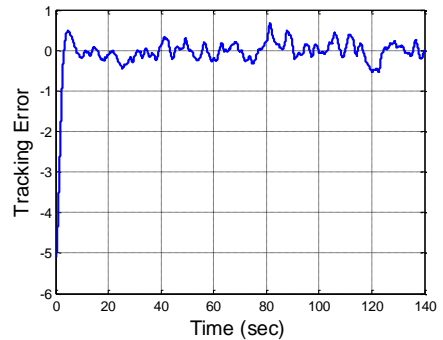


Figure 10. Roll Angle Tracking error

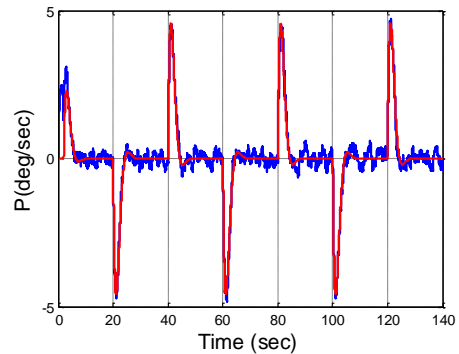


Figure 11. Roll Rate Tracking Performance (σ -modification)

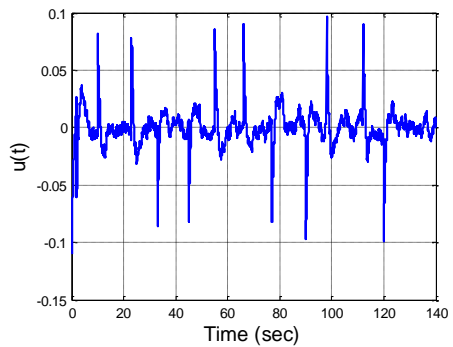


Figure 12. Control Signal

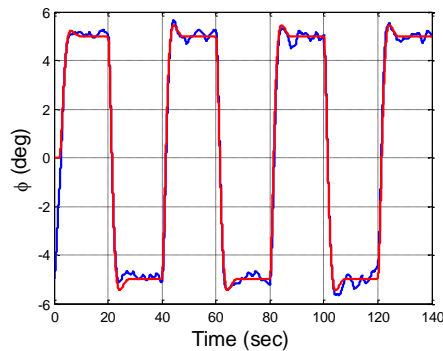


Figure 13. Roll Angle Tracking (e-modification)

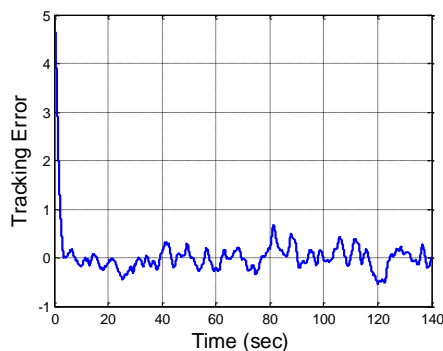


Figure 14. Roll Angle Tracking error

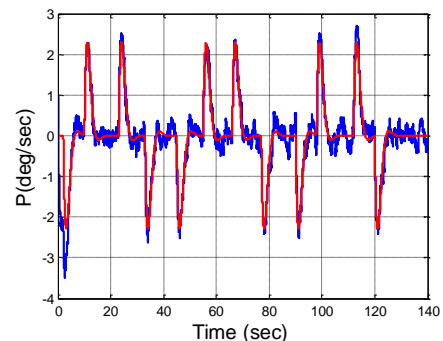


Figure 15. Roll Rate Tracking Performance (e-modification)

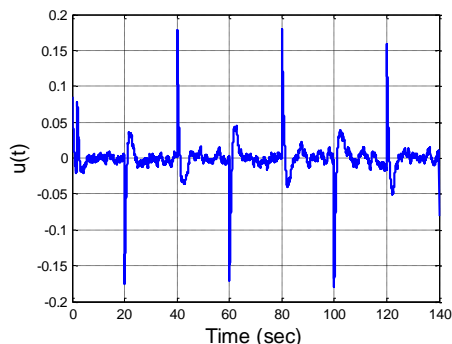


Figure 16. Control Signal

6. CONCLUSION

In this study, we proposed a general adaptive laws for MRAC and Robust MRAC schemes. In the simple MRAC structure, the adaptive laws derived from these type of Lyapunov function could be considered as an adaptive law which derived from common quadratic Lyapunov function with variable adaptation gains. This method can be applied to design Dead-zone modification and projection-based MRAC systems. The proposed Lyapunov function can be applied to design adaptive controllers designed by the Lyapunov's direct method.

7. REFERENCES

- Gursul, I., Wang, Z., "Flow control of tip/edge vortices", *AIAA Journal*, Vol. 56, No. 5, (2018), 1731-1749, doi: 10.2514/1.J056586.
- Chen, K., Dong, Y., Shi, Z., Tong, S. X., & Sha, J., "Experimental Study of the Suppression of Wing-Body Rock by Spanwise Blowing" In 2019 IEEE 10th International Conference on Mechanical and Aerospace Engineering (2019), 142-146. Doi: 10.1109/ICMAE.2019.8880951.
- Katz, J., "Wing/vortex interactions and wing rock", *Progress in Aerospace Sciences*, Vol. 35, No. 7, (1999), 727-750, doi: 10.1016/S0376-0421(99)00004-4.
- Ma, B. F., Wang, Z., Gursul, I. "Symmetry breaking and instabilities of conical vortex pairs over slender delta wings", *Journal of Fluid Mechanics*, Vol. 832, (2017), 41-72, doi: 10.1017/jfm.2017.648.
- Ma, B., Deng, X., Wang, B., "Effects of wing locations on wing rock induced by forebody vortices", *Chinese Journal of Aeronautics*, Vol. 29, No. 5, (2016), 1226-1236, doi: 10.1016/j.cja.2016.08.004.
- Gursul, I., Xie, W., "Origin of vortex wandering over delta wings", *Journal of Aircraft*, Vol. 37, No. 2, (2000), 348-350, doi: 10.2514/2.2603.
- Ericsson, L. E., "Various sources of wing rock", *Journal of Aircraft*, Vol. 27, No. 6, (1990), 488-494, Doi: 10.2514/3.25309.
- Jun, Y.W., Nelson, R.C., "Leading-edge vortex dynamics on a slender oscillating wing", *Journal of Aircraft*, Vol. 25, No. 9, (1988), 815-819, doi: 10.2514/3.45664.
- Nguyen, L., Yip, L., Chambers, J., "Self-induced wing rock of slender delta wings", In *7th Atmospheric Flight Mechanics Conference*, (1981), 1883, doi: 10.2514/6.1981-1883.
- Ma, B. F., Wang, B., Deng, X. Y., "Effects of Reynolds numbers on wing rock induced by forebody vortices", *AIAA Journal*, Vol. 55, No. 9, (2017), 2980-2991, doi: 10.2514/1.J055461.
- Hsu, C. H., Lan, C. E., "Theory of wing rock", *Journal of Aircraft*, Vol. 22, No. 10, (1985), 920-924, doi: 10.2514/3.45225.
- Nayfeh, A. H., Elzebda, J. M., Mook, D. T., "Analytical study of the subsonic wing-rock phenomenon for slender delta wings", *Journal of Aircraft*, Vol. 26, No. 9, (1989), 805-808, doi: 10.2514/3.45844.
- Elzebda, J. M., Nayfeh, A. H., Mook, D. T., "Development of an analytical model of wing rock for slender delta wings", *Journal of Aircraft*, Vol. 26, No. 8, (1989), 737-743, doi: 10.2514/3.45833.
- Go, T. H., "Aircraft wing rock dynamics and control", Doctoral Dissertation, Massachusetts Institute of Technology, (1999).

15. Hsu, C. F., Lin, C. M., Chen, T. Y., "Neural-network-identification-based adaptive control of wing rock motions", *IEEE Proceedings-Control Theory and Applications*, Vol. 152, No.1, (2005), 65-71, doi: 10.1049/ip-cta:20050904.
16. Liu, Z. L., "Reinforcement adaptive fuzzy control of wing rock phenomena", *IEEE Proceedings-Control Theory and Applications*, Vol. 152, No. 6, (2005), 615-620, doi: 10.1049/ip-cta:20045072.
17. Tao, C. W., Taur, J. S., Chang, C. W., Chang, Y. H., "Simplified type-2 fuzzy sliding controller for wing rock system", *Fuzzy Sets and Systems*, Vol. 207, (2012), 111-129, doi: 10.1016/j.fss.2012.02.015.
18. Lin, C. M., Hsu, C. F., "Supervisory recurrent fuzzy neural network control of wing rock for slender delta wings", *IEEE Transactions on Fuzzy Systems*, Vol. 12, No. 5, (2004), 733-742, doi: 10.1109/TFUZZ.2004.834803.
19. Monahemi, M., Barlow, J., Krstic, M., "Control of wing rock motion of slender delta wings using adaptive feedback linearization", In Guidance, Navigation, and Control Conference, (1995), 3344, doi: 10.2514/6.1995-3344.
20. Araujo, A. D., Singh, S. N., "Variable structure adaptive control of wing-rock motion of slender delta wings", *Journal of Guidance, Control, and Dynamics*, Vol. 21, No. 2, (1998), 251-256, doi: 10.2514/2.4250.
21. Arab Markadeh, G. R., Soltani, J., "A Current-Based Output Feedback Sliding Mode Control for Speed Sensorless Induction Machine Drive Using Adaptive Sliding Mode Flux Observer", *International Journal of Engineering, Transactions A: Basics*, Vol. 19, No. 1, (2006), 21-34.
22. Karami-Mollaei, A., "Adaptive Fuzzy Dynamic Sliding Mode Control of Nonlinear Systems", *International Journal of Engineering, Transactions B: Applications*, Vol. 29, No. 8, (2016) 1075-1086, doi: 10.5829/idosi.ije.2016.29.08b.07.
23. Sadeghijaleh, M., Fateh, M.M., "Adaptive Voltage-based Control of Direct-drive Robots Driven by Permanent Magnet Synchronous Motors", *International Journal of Engineering, Transactions A: Basics*, Vol. 30, No. 4, (2017), 507-515, doi: 10.5829/idosi.ije.2017.30.04a.08.
24. Malekzadeh, M., Shahbazi, B., "Robust Attitude Control of Spacecraft Simulator with External Disturbances", *International Journal of Engineering, Transactions A: Basics*, Vol. 30, No. 4, (2017), 567-574, doi: 10.5829/idosi.ije.2017.30.04a.15.
25. Gholipour, R., Fateh, M. M., "Designing a Robust Control Scheme for Robotic Systems with an Adaptive Observer", *International Journal of Engineering, Transactions B: Applications*, Vol. 32, No. 2, (2019), 284-291, doi: 10.5829/ije.2019.32.02b.12.
26. Manouchehri, P., Ghasemi, R., Toloee, A., "Distributed Fuzzy Adaptive Sliding Mode Formation for Nonlinear Multi-quadrotor Systems", *International Journal of Engineering, Transactions B: Applications*, Vol. 33, No. 5, (2020), 798-804, doi: 10.5829/IJE.2020.33.05B.11.
27. Rao, M. P. R. V., "Non-quadratic Lyapunov function and adaptive laws for model reference adaptive control", *Electronics Letters*, Vol. 34, No. 23, (1998), 2278-2280, doi: 10.1049/el:19981503.
28. Hassan, H. A., Rao, M. P. R. V., "Novel Robust Adaptive Control Scheme Using Non-Quadratic Lyapunov Functions For Higher Order Systems", In EUROCON The International Conference on Computer as a Tool IEEE (2005), Vol. 1, 286-289, doi: 10.1109/EURCON.2005.1629917.
29. Hosseinzadeh, M., Yazdanpanah, M. J., "Performance enhanced model reference adaptive control through switching non-quadratic Lyapunov functions", *Systems & Control Letters*, Vol. 76, (2015), 47-55, doi: 10.1016/j.sysconle.2014.12.001.
30. Lavretsky, E., Wise, K.A., "Robust and adaptive control", Springer, London, (2013), doi: 10.1007/978-1-4471-4396-3.

8. APPENDIX

8.1. Appendix A Let $\phi \neq M \subset \mathbb{R}^n$ be an open set, Let $\phi \neq N \subset M$ be a compact and convex set and let $f \in C^1(M, \mathbb{R})$ be a function. We prove that f is Lipschitz on N , in other words there exists $\alpha > 0$ such that

$$|f(x) - f(y)| \leq \alpha \|x - y\| \quad \forall x, y \in N \quad (\text{A.1})$$

By definition:

$$\rho(t): [0,1] \rightarrow N \quad (\text{A.2})$$

ρ is the line segment between x, y . so we have:

$$\rho(0) = x \quad (\text{A.3})$$

$$\rho(1) = y \quad (\text{A.4})$$

$$\rho'(t) = (y - x) \quad (\text{A.5})$$

Since N is convex so $\rho(t)$ lies entirely in N , hence in M . For $x, y \in N$ we have:

$$\|f(y) - f(x)\| = \left\| \int_0^1 \frac{df(\rho(t))}{dt} dt \right\| \cdot \left\| \int_0^1 \nabla f(\rho(t)) \rho'(t) dt \right\| \leq \int_0^1 \|\nabla f(\rho(t)) \rho'(t)\| dt \leq \int_0^1 \|\nabla f(\rho(t))\| \|\rho'(t)\| dt \quad (\text{A.6})$$

Since N is compact and $\nabla f \in C^0(M, \mathbb{R})$ so $\nabla f \in C^0(N, \mathbb{R})$, $\|\nabla f\|$ is bounded by some α on N so:

$$\int_0^1 \|\nabla f(\rho(t))\| \|\rho'(t)\| dt \leq \int_0^1 \alpha \|\rho'(t)\| dt \quad (\text{A.7})$$

Using (A.5) yields:

$$\int_0^1 \alpha \|\rho'(t)\| dt = \int_0^1 \alpha \|y - x\| dt = \alpha \|y - x\| \quad (\text{A.8})$$

Using (A.6), (A.7), and (A.8) yields:

$$\|f(y) - f(x)\| \leq \alpha \|y - x\| \quad (\text{A.9})$$

8.2. Appendix B

By definition:

$$[a, b] = \frac{f(a) - f(b)}{a - b} \quad (\text{B.1})$$

Using mean-value theorem yields:

$$\tau \in (a, b) \rightarrow f'(\tau) = [a, b] \quad (\text{B.2})$$

For $a < b < c$ we have:

$$|[a, b] - [b, c]| = |f'(\tau_1) - f'(\tau_2)| \leq L|a - c| \quad (\text{B.3})$$

Which proves boundedness of second-time derivative or 2-Lipschitz continuity of the function f .

Persian Abstract

چکیده

روش مستقیم لیاپانف یک از ابزارهای مهم طراحی سیستم های تطبیقی مدل مرجع و تطبیقی مقاوم می باشد. در حالت کلی تابع لیاپانف کاندید شامل ۲ دسته از عبارت های مربعی می باشد. اولین دسته شامل خطای تعقیب حالت و یا در حالت های خاص شامل حالت سیستم می باشد. دسته دوم شامل عبارت های مربعی خطای تخمین پارامترهای کنترلر می باشد. برای طراحی سیستم های تطبیقی مدل مرجع و تطبیقی مقاوم پژوهشگران تنوع محدودی در انتخاب توابع مربعی به کار برده اند. در این پژوهش، یک حالت کلی برای عبارت مربعی شامل متغیر خطای حالت تعقیب در نظر می گیریم. یک تابع دلخواه اکیدا صعودی که متعلق به توابع کلاس C^1 بوده و تابعی از چند جمله ای های مربعی خطای تعقیب حالت بوده در نظر گرفته می شود. با این انتخاب یک ساختار کلی برای قوانین تطبیق پارامترهای کنترلر بدست آورده می شود. برای سیستم مدل مرجع اثبات پایداری مجانبی فراگیر سیستم حلقه بسته و برای الگوریتم های تطبیقی مقاوم اثبات پایداری و ردیابی یکنواخت کراندار تضمین می گردد. در نهایت با هدف ارزیابی عملکرد کنترلرهای طراحی شده سیستم یک درجه آزادی پدیده وینگ راک در نظر گرفته شده است.
